115 W fiber laser with all solid-structure and large-mode-area multicore fiber

JUNHUA JI,[1] SIDHARTHAN RAGHURAMAN,[1] XIAOSHENG HUANG,[1] JICHAO ZANG,[1] DARYL HO,[1] YANYAN ZHOU,[1] YEHUDA BENUDIZ,[2], UDI BEN AMI,[2] AMIEL A. ISHAAYA,[2] SEONGWOO YOO[1,*]

[1] *School of Electrical and Electronic Engineering, Centre of Optical Fibre Technology, The Photonics Institute, Nanyang Technological University, 50 Nanyang Avenue, 639798, Singapore*
[2]*Department of Electrical and Computer Engineering, Ben-Gurion University of the Negev, Beer-Sheva 84105, Israel*
**Corresponding author: seon.yoo@ntu.edu.sg*

Received XX Month XXXX; revised XX Month, XXXX; accepted XX Month XXXX; posted XX Month XXXX (Doc. ID XXXXX); published XX Month XXXX

We investigate mode area scaling by means of supermode operation in an all-solid multicore fiber. To obtain a large mode area, we designed and fabricated an active double-clad multicore fiber, where each Ytterbium-doped core is 19 μm in diameter and has a numerical aperture of 0.067, comparable to the core of the largest available commercial large-mode-area (LMA) fibers. Such six large cores are stacked tightly in a ring structure to enable phase locking of the core fields and supermode operation. The fiber laser performance was investigated in a linear laser cavity with an external Talbot resonator for mode selection. The highest output power achieved was 115 W with an overall 61% slope efficiency corresponding to the pump power. The measured M^2 was 1.43 for the central lobe with nearly 70% of the total power. © 2015 Optical Society of America

OCIS codes: *(140.3510) Lasers, fiber; (140.3290) Laser arrays; (060.2280) Fiber design and fabrication*

A large mode area fiber is a key component in high power fiber lasers, helping mitigatevarious unwanted effects, e.g. nonlinear effects and transverse mode instability (TMI) [1-3] . It is viewed that an effective area of the fundamental mode (FM) is limited to about 1000 μm^2 since the effective-index difference between the FM and higher-order modes (HOMs) becomes smaller as the mode area increases. Various specialty LMA fiber designs are reported to overcome the challenge, through selective doping [4], or mode-differentiated losses, e.g., chirally-coupled core (CCC) fibers [5], leaky channel fibers (LCFs) [6], large-pitch photonic-crystal fibers (LPFs) [7], multi-trench fibers (MTFs) [8], or asymmetric core fibers [9, 10]. Recently, multi-core fibers (MCFs) have been investigated as a platform of the spatial division multiplexing for increasing optical communication bandwidth [11, 12]. Individual cores in the MCF are separated enough to prevent cross-talk. Alternatively, the cores can be place closely in an attempt to achieve phase locking and coherent beam combing (CBC). The CBC of fiber lasers has been intensively investigated over the past since it is a promising approach to overcome these limitations and allow further scaling of output power or energy [13,14]. The MCFs with closely packed cores can be used as a platform for CBC of beams from separate cores, due to the common environment (heat, gain) among the cores that inherently reduces possible phase fluctuation. When multiple cores are close enough, supermodes are formed through evanescent field coupling between adjacent cores. Usually the in-phase supermode is intentionally selected to lase since it has a central bright lobe in the far field, and the beam quality of the central lobe is nearly diffraction-limited, better than that of other supermodes. Various methods have been proposed and demonstrated for the selection of the in-phase mode, e.g., with a Talbot mirror as a laser cavity mirror [15-18], through selective injection [19, 20] or by placing an aperture inside the laser cavity [21]22. However, most of the work done with large-mode-area (LMA) cores [16], [18], [21] were based on multi-core photonic crystal fibers (PCF), which are relatively complex and costly to fabricate, and challenging in terms of handling (cleaving and splicing). On the other hand, for those MCFs with all-solid structures, the core sizes were relatively small, hence offering limited mode area scaling [15], [17],[19], [20], [22]

In this paper, we introduce an alternative all-solid MCF design with large nearly single-mode core size, i.e., 19 μm core diameter and 0.067 core numerical aperture (NA), which was in-house fabricated. To the best of our knowledge, this is the largest active LMA core in a multicore fiber with all-solid structure ever reported. Our MCF has six cores aligned in a ring shape. The performance of the fabricated MCF is investigated in a linear laser cavity with an external Talbot mirror to select the in-phase mode. At full pump power, the signal output power was 115 W with the slope efficiency of 61% with respect to the pump power. The measured M^2 of the

output signal beam, with or without filtering out the pedestal, was 1.34 and 3.34, respectively.

The fiber was fabricated with the standard *stack and draw* method. We etched the cladding layer of an Yb-doped fiber preform made by a conventional modified chemical vapor deposition (MCVD) process with a rare-earth vapor delivery system, cut it into six pieces, and placed them in a ring configuration at the center of the multi-core fiber preform. Theoretically, MCFs with hexagonal ring structure has best performance in terms of power handling and good output beam quality compared to that of MCFs with hexagonal structure or squared array [23]. The fiber preform was then drawn into an all-solid fiber with a low index polymer jacket. The image of the center cross-section of the MCF measured by a microscope is shown in Fig. 1(a). Each core diameter is ~19 μm. Figure 1(b) shows the measured refractive index profile (RIP) of the MCF along the diagonal. The measured NA is about 0.067 (very similar to the available commercial LMA fibers). Each core is slightly multimoded at ~1 μm. The cladding diameter is ~235 μm with NA of 0.45. The measured small signal absorption is about 4 dB/m at the 976 nm absorption peak.

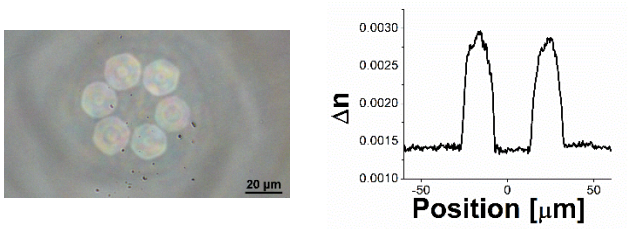

(a) (b)

Fig. 1. (a) Image of the Yb-doped MCF, (b) Refractive index profile of the MCF along the diagonal.

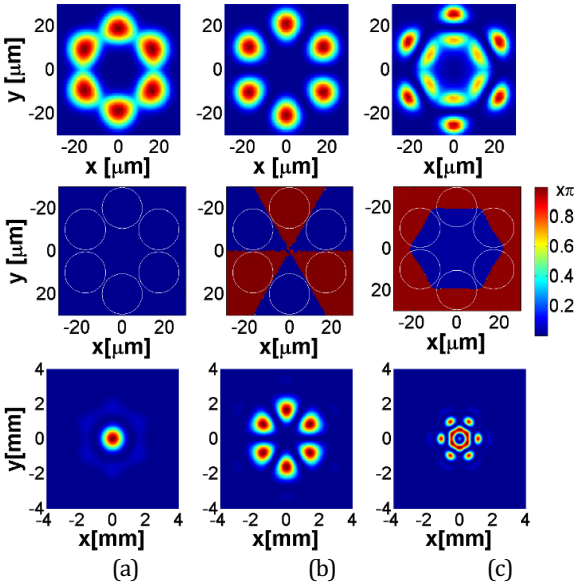

(a) (b) (c)

Fig. 2. Mode distributions at near field (row 1) and far field with z = 50 mm (row 3) and phase distributions (row 2): (a) in-phase mode; (b) out-of-phase mode; (c) one example of higher-order modes.

We used the commercial software COMSOL to simulate the mode distribution. In the first row of Fig. 2, it shows mode distributions of three examples, i.e., fundamental in-phase mode, fundamental out-of-phase mode and a higher order supermode. The calculated effective mode area of the fundamental in-phase mode is 1571 μm^2, which is corresponding to the mode field diameter (MFD) of ~45 μm in a step-index fiber. Since the field distribution of each mode in the fiber has been calculated, the corresponding far field intensity distribution after a propagation distance can be obtained by numerically solving the Fresnel diffraction integral using a standard fast Fourier transform (FFT) method [24]. The intensity distributions of these three modes at far field with z=50 mm are shown in the third row of Fig. 2. The far-field pattern of the fundamental in-phase mode has a dominant central lobe, different from its near-filed distribution. The calculated power in the central lobe is 68.4% of the total in-phase mode power. The mode distribution of the out-of-phase remains almost same along the propagation. The phase distribution of three modes are shown in the second row of Fig. 2. The phase remains same in separate cores for in-phase mode while the phase difference changes π between two adjacent cores for the out-of-phase mode. With the mode distribution along z, the beam qualities of three mode can be calculated as M^2 = 2.8, 5.4, and 6.6, respectively for the fundamental in-phase mode, out-of-phase mode and the HOM through the second-moment beam width [25]. The reason why we gave the example of the HOM here will be explained in the discussion of the experimental results.

A 3.5 m long Yb-doped MCF was investigated in a linear laser cavity with a bending diameter of ~25 cm. Figure 3 shows the schematics of the experimental setup. The MCF was cladding-pumped by a fiber-coupled laser diode at 976 nm (not wavelength stabilized) through the flat-cleaved end via lenses and dichroic mirrors (DMs). A high reflection (HR) mirror was placed close to the other fiber end as a Talbot mirror. The excited supermodes can be selected by moving the HR mirror backward and forward. The output beam profile of the fiber laser at the far field was recorded with a camera which was directly placed 50 mm from the fiber end, behind the HR mirror.

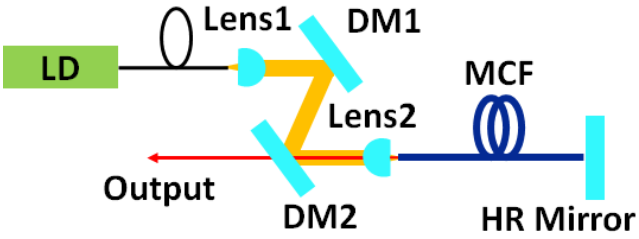

Fig. 3. The schematic diagram of the experimental setup. DM: dichroic mirror; HR Mirror: high reflection mirror; MCF: multi-core fiber.

The far-field intensity beam distributions captured by the camera were compared to the calculated ones as shown in Fig. 4. The calculated beam distributions of the fundamental in-phase mode and out-of-phase mode are given in Fig. 4(a) and Fig. 4(c), respectively, assuming that the beam propagates 50 mm from the fiber end. Fig. 4(b) and Fig. 4(d) show the measured beam distribution with the distances between HR mirror and fiber end of

~2 mm and <1 mm, respectively. When the distance between the HR mirror and fiber end is 2 mm, the measured beam distribution is very similar to the beam profile of the fundamental in-phase mode indicating that the in-phase mode was excited and dominated the lasing in this case. The measured power in the central lobe is about 72% of the total power, very close to the calculated central lobe power ratio of the fundamental in-phase mode, i.e., 68.4%. By moving the HR mirror closer to the fiber end, i.e., <1 mm, the measured beam profile became donut shaped, as shown in Fig. 4(d). As evident, it is different from the calculated beam profile of the fundamental output-of-phase supermode, indicating that the out-of-phase mode didn't dominate the lasing.

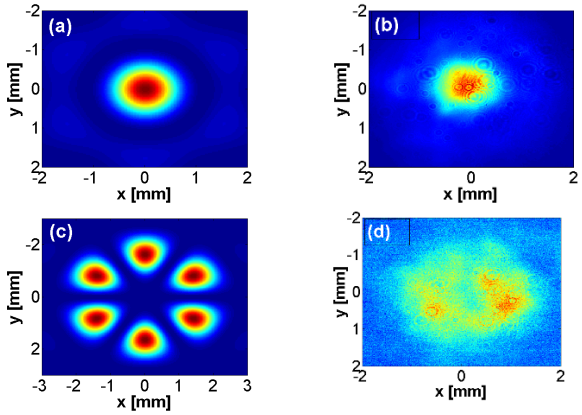

Fig. 4. Calculated (a,c) and measured (b,d) far-field intensity distributions. (a, b) are the in-phase supermode; (c) is the calculated out-of-phase mode; and (d) is the measured far field when the HR mirror is <1 mm from the fiber end.

The position of the HR mirror was fixed at ~2 mm away from the fiber end for the selection of the fundamental in-phase mode. The measured output power as a function of the pump power is shown in Fig. 5. The measured data is given in black dots while the red dashed line is the fitting curve. The laser started to lase with output power of 0.88 W at 9 W pump power. The highest output signal is 115 W at pump power of 198.6 W. The output power is limited by the available pump power. The overall slope efficiency with respect to the laser diode pump power is ~61.4%. We measured the beam quality of the output signal at full pump power. The measured M^2 is ~3.34, which is comparable to the theoretical M^2 value of the fundamental in-phase mode, i.e., 2.8. An adjustable aperture was then placed at the output to carefully filter out the pedestal as shown in Fig. 4(a) by monitoring the beam distribution on the camera. The measured M^2 without pedestal is given in Fig. 6. The blue crosses and black squares are the measured results for along x and y axis, respectively. The red dashed line and straight line are corresponding fitting curves. By filtering out the pedestal, the measured M^2 is ~1.43, close to the beam quality of the diffraction limited beam.

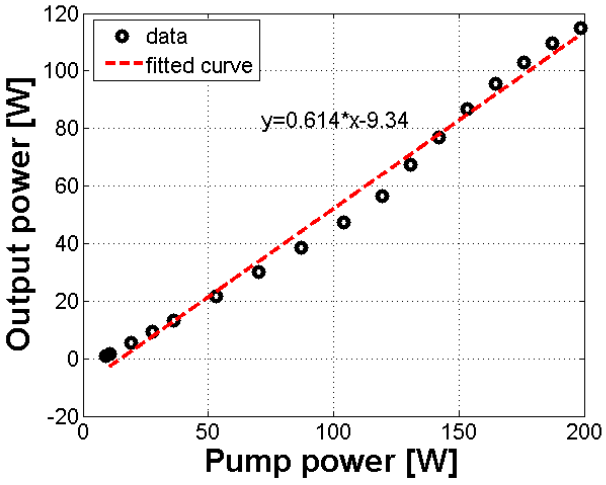

Fig. 5. Laser output power vs. pump power.

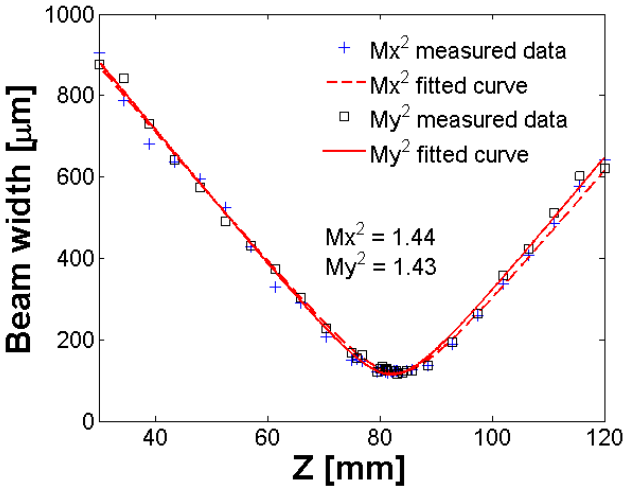

Fig. 6. Beam quality measured at full pump power.

To better understand the experimental results, we calculated the amplitude coupling coefficients of different supermodes in the Talbot resonator. The calculated results are given in Fig. 7. All the solid curves present the coupling coefficient of each mode to couple back into itself after it propagates between the fiber end and HR mirror and returns back to the fiber end. The red dashed line plots the amplitude coupling coefficient of the fundamental mode coupling into the higher order mode given in Fig. 2(c). Note that the coupling losses at distances larger than 0.2mm are relatively large due to diffraction. The results are very similar to those reported in the literature, e.g. [26]. We also have three regimes for mode selection due to Talbot effect. When the distance between the HR mirror and the fiber is longer than ~0.7 mm, the amplitude coupling coefficient of the fundamental in-phase mode given in solid black curve is highest among all modes. This is expected since the diffraction angle of the fundamental in-phase mode is lowest. It also can explain that in our experiment, the fundamental in-phase mode was excited and dominated the lasing when the HR mirror was put at the position of 2 mm away from the fiber end. However, since each Yb-doped core is slightly multimoded, there exist higher order modes. By calculations, we notice that in this regime, the

fundamental in-phase mode can be strongly coupled into the higher order supermode given in the red dashed line in Fig. 2(c). We attribute this to the degradation of the output beam quality as the measured beam quality of the output signal is slightly worse than the theoretical number. To eliminate the coupling coefficient from the fundamental in-phase supermode into such higher order mode, we should make sure that each core in the fiber is truly single-moded. When the fiber-HR mirror distance is shorter than 0.3 mm, the amplitude coupling coefficients of all modes coupled into themselves are close. The coupling efficient of the in-phase mode is only slightly higher than the others. When the fiber-HR distance is between 0.3 mm and 0.7 mm, another higher order supermode has a slightly higher coupling coefficient than the other modes. This can explain the multimode operation we observed in this case as shown in Fig. 4(d). The measured mode distribution is different from the calculated mode profile of the out-of-phase supermode.

In conclusion, we investigated mode area scaling via an all-solid MCF with Yb-doped LMA cores fabricated in-house. The effective area of the fundamental in-phase mode can be as large as 1571 μm^2, corresponding to ~45 μm MFD of a conventional step-index fiber. The fabricated MCF was then investigated in a linear cavity with Talbot effects. The output beam quality of central lobe is nearly diffraction limited with measured M^2 of 1.43. The maximum output power obtained was 115 W, limited by available pump power. By calculation of the amplitude coupling coefficients of the various supermodes, we observe that the fundamental in-phase mode has lower coupling losses than other modes when the distance between the HR mirror and the fiber end is larger than 0.7mm. In the future, we will try to introduce additional external means to try and operate the laser with the out-of-phase mode. Besides, we will fabricate MCFs with LMA and single-moded cores.

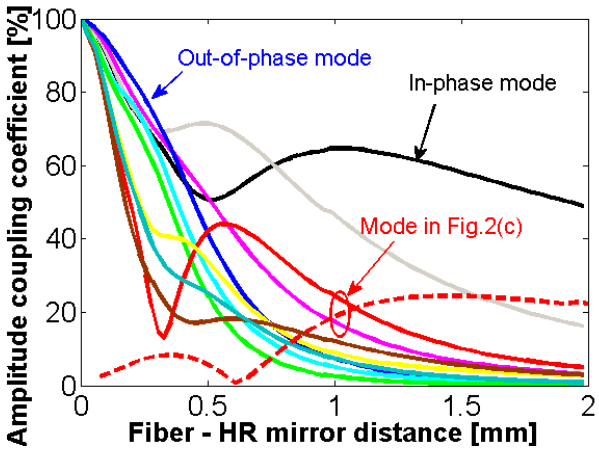

Fig. 7. Amplitude coupling coefficients of different supermodes as a function of the fiber-HR mirror distance.

Acknowledgment. The authors wish to acknowledge the Tan Chin Tuan Fellowship that allowed the initial collaboration with the research groups between Ben-Gurion University of the Negev and Nanyang Technological University.

References

1. D. J. Richardson, J. Nilsson, and W. A. Clarkson, J. Opt. Soc. Am. B **27**, B63(2010).
2. H.-J. Otto, C. Jauregui, J. Limpert, A. Tünnermann, in *Proc. SPIE 9728, Fiber Lasers XIII: Technology, Systems, and Applications 2016*, p. 97280E.
3. J. Zhu, P. Zhou, Y. Ma, X. Xu, and Z. Liu, Opt. Express **19**, 18645(2011).
4. J. R. Marciante, *IEEE J. Sel. Top. Quantum Electron.* **15**, 30 (2009).
5. X. Ma, C. Zhu, I-N. Hu, A. Kaplan, and A. Galvanauskas, Opt. Express **22**, 9206 (2014).
6. L. Dong, T. W. Wu, H. A. McKay, L. Fu, J. Li, and H. G. Winful, *IEEE J. Sel. Top. Quantum Electron.* **15**, 47 (2009).
7. J. Limpert, F. Stutzki, F. Jansen, H. J. Otto, T. Eidam, C. Jauregui, and A. Tünnermann, *Light: Sci. & App.* **1**, 1 (2012).
8. D. Jain, C. Baskiotis, and J. K. Sahu, *Opt. Express* **21**, 1448 (2013).
9. B. Anderson, G. Venus, D. Ott, I. Divliansky, J. W. Dawson, D. R. Drachenberg, M. J. Messerly, P. H. Pax, J. B. Tassano, and L. B. Glebov, *Opt. Lett.* **39**, 6498 (2014).
10. N. Xia, and S. Yoo, *Opt. Express* **25**, 13230 (2017).
11. R. G. H. van Uden, R. A. Correa, E. A. Lopez, F. M. Huijskens, C. Xia, G. Li, A. Schülzgen, H. de Waardt, A. M. J. Koonen, and C. M. Okonkwo, Nature Photonics **8**, 865 (2014).
12. T. Sakamoto, T. Matsui, K. Saitoh, S. Saitoh, K. Takenaga, T. Mizuno, Y. Abe, K. Shibahara, Y. Tobita, S. Matsuo, K. Aikawa, S. Aozasa, K. Nakajima, and Y. Miyamoto, J. Lightwave Technol. **35**, 443 (2017).
13. Z. Liu, P. Ma, R. Su, R. Tao, Y. Ma, X. Wang, and P. Zhou, J. Opt. Soc. Am. B **34**, A7(2017).
14. T. Y. Fan, IEEE Journal of Selected Topics in Quantum Electronics **11**, 567(2005).
15. M. Wrage, P. Glas, D. Fischer, M. Leitner, D. V. Vysotsky, and A. P. Napartovich, Opt. Lett. **25**, 1436(2000).
16. L. Michaille, C. R. Bennett, D. M. Taylor, T. J. Shepherd, J. Broeng, H. R. Simonsen, and A. Petersson, Opt. Lett. **30**, 1668-1670(2005).
17. L. Li, A. Schülzgen, H. Li, V. L. Temyanko, J. V. Moloney, and N. Peyghambarian, J. Opt. Soc. Am. B **24**, 1721(2007).
18. A. Shirakawa, T. Kobayashi, M. Matsumoto and K-i. Ueda, in *proceedings of CLEO/QELS: 2010 Laser Science to Photonic Applications 2010* (Optical Society of America, 2012), p. 1.
19. J. Lhermite, E. Suran, V. Kermene, F. Louradour, A. Desfarges-Berthelemot, and A. Barthélémy, Opt. Express **18**, 4783(2010).
20. B. M. Shalaby, V. Kermène, D. Pagnoux, A. Desfarges-Berthelemot, A. Barthélémy, A. Popp, M. Abdou Ahmed, A. Voss, and T. Graf, Appl. Phys. B **100**, 859(2010).
21. X. Fang, M. Hu, C. Xie, Y. Song, L. Chai, and C. Wang, Opt. Lett. **36**, 1005(2011).
22. L. Li, A. Schülzgen, S. Chen, V. L. Temyanko, J. V. Moloney, and N. Peyghambarian, Opt. Lett. **31**, 2577 (2006).
23. P. Zhou, X. Wang, Y. Ma, H. Ma, X. Xu and Z. Liu, Chinese Phys. Lett. **26**, 084205-1(2009).
24. Y. Li and T. Erdogan, Opt. Commun. **183**, 377(2000).
25. A. E. Siegman, in *Proc. SPIE 1810, 9th International Symposium on Gas Flow and Chemical Lasers 1993*, p. 758.
26. L. Michaille, C. R. Bennett, D. M. Taylor and T. J. Shepherd, IEEE Journal of Selected Topics in Quantum Electronics **15**, 328(2009).

Full References

1. D. J. Richardson, J. Nilsson, and W. A. Clarkson, "High power fiber lasers: current status and future perspectives [Invited]," J. Opt. Soc. Am. B, vol. 27, no. 11, pp. B63-B92, 2010.
2. H.-J. Otto, C. Jauregui, J. Limpert, A. Tünnermann, "Average power limit of fiber-laser systems with nearly diffraction-limited beam quality," Proc. SPIE 9728, Fiber Lasers XIII: Technology, Systems, and Applications, 97280E, 9 March 2016.
3. J. Zhu, P. Zhou, Y. Ma, X. Xu, and Z. Liu, "Power scaling analysis of tandem-pumped Yb-doped fiber lasers and amplifiers," Opt. Express, vol. 19, no. 19, pp. 18645-18654, 2011.
4. J. R. Marciante, "Gain filtering for single-spatial-mode operation of large-mode-area fiber amplifiers," *IEEE J. Sel. Top. Quantum Electron.*, vol. 15, no. 1, pp. 30-36, 2009.
5. X. Ma, C. Zhu, I-N. Hu, A. Kaplan, and A. Galvanauskas, "Single-mode chirally-coupled-core fibers with larger than 50μm diameter cores," Opt. Express 22, 9206-9219 (2014)
6. L. Dong, T. W. Wu, H. A. McKay, L. Fu, J. Li, and H. G. Winful, "All-glass large-core leakage channel fibers," *IEEE J. Sel. Top. Quantum Electron.*, vol. 15, no. 1, pp. 47-53, 2009.
7. J. Limpert, F. Stutzki, F. Jansen, H. J. Otto, T. Eidam, C. Jauregui, and A. Tünnermann, "Yb-doped large-pitch fibers: effective single-mode operation based on higher-order mode delocalization," *Light: Sci. & App.*, vol. 1, pp. 1-5, 2012.
8. D. Jain, C. Baskiotis, and J. K. Sahu, "Mode area scaling with multi-trench rod--," *Opt. Express*, vol. 21, no. 2, pp. 1448-1455, 2013.
9. B. Anderson, G. Venus, D. Ott, I. Divliansky, J. W. Dawson, D. R. Drachenberg, M. J. Messerly, P. H. Pax, J. B. Tassano, and L. B. Glebov, "Fundamental mode operation of a ribbon fiber laser by way of volume Bragg gratings," *Opt. Lett.*, vol. 39, no. 22, pp. 6498-6500, 2014.
10. N. Xia, and S. Yoo, "Mode instability in ytterbium-doped non-circular fibers," *Opt. Express*, vol. 25, no. 12, pp. 13230-13251, 2017.
11. R. G. H. van Uden, R. Amezcua Correa, E. Antonio Lopez, F. M. Huijskens, C. Xia, G. Li, A. Schülzgen, H. de Waardt, A. M. J. Koonen, and C. M. Okonkwo, "Ultra-High-Density Spatial Division Multiplexing with a Few-Mode Multicore Fibre", Nature Photonics 8 (11), pp. 865-870.
12. Taiji Sakamoto, Takashi Matsui, Kunimasa Saitoh, Shota Saitoh, Katsuhiro Takenaga, Takayuki Mizuno, Yoshiteru Abe, Kohki Shibahara, Yuki Tobita, Shoichiro Matsuo, Kazuhiko Aikawa, Shinichi Aozasa, Kazuhide Nakajima, and Yutaka Miyamoto, "Low-Loss and Low-DMD 6-Mode 19-Core Fiber With Cladding Diameter of Less Than 250 μm," J. Lightwave Technol. 35, 443-449 (2017).
13. Z. Liu, P. Ma, R. Su, R. Tao, Y. Ma, X. Wang, and P. Zhou, "High-power coherent beam polarization combination of fiber lasers: progress and prospect [Invited]," J. Opt. Soc. Am. B, vol. 34, no. 3, pp. A7-A14, 2017.
14. T. Y. Fan, "Laser beam combining for high-power, high-radiance sources," IEEE Journal of Selected Topics in Quantum Electronics, vol. 11, no. 3, pp. 567-577, 2005.
15. M. Wrage, P. Glas, D. Fischer, M. Leitner, D. V. Vysotsky, and A. P. Napartovich, "Phase locking in a multicore fiber laser by means of a Talbot resonator," Opt. Lett., vol. 25, no. 19, pp. 1436-1438, 2000.
16. L. Michaille, C. R. Bennett, D. M. Taylor, T. J. Shepherd, J. Broeng, H. R. Simonsen, and A. Petersson, "Phase locking and supermode selection in multicore photonic crystal fiber lasers with a large doped area," Opt. Lett., vol. 30, no. 13, pp. 1668-1670, 2005.
17. L. Li, A. Schülzgen, H. Li, V. L. Temyanko, J. V. Moloney, and N. Peyghambarian, "Phase-locked multicore all-fiber lasers: modeling and experimental investigation," J. Opt. Soc. Am. B, vol. 24, no. 8, pp. 1721-1728, 2007.
18. A. Shirakawa, T. Kobayashi, M. Matsumoto and K-i. Ueda, "All-fiber phase-locked multi-core photonic crystal fiber laser with fill-factor enhancement and high efficiency," in proceedings of CLEO/QELS: 2010 Laser Science to Photonic Applications, San Jose, CA, 2010, pp. 1-2.
19. J. Lhermite, E. Suran, V. Kermene, F. Louradour, A. Desfarges-Berthelemot, and A. Barthélémy, "Coherent combining of 49 laser beams from a multiple core optical fiber by a spatial light modulator," Opt. Express, vol. 18, no. 5, pp. 4783-4789, 2010.
20. B. M. Shalaby, V. Kermène, D. Pagnoux, A. Desfarges-Berthelemot, A. Barthélémy, A. Popp, M. Abdou Ahmed, A. Voss, and T. Graf, "19-cores Yb-fiber laser with mode selection for improved beam brightness," Appl. Phys. B, vol. 100, no. 4, pp. 859-864, 2010.
21. L. Li, A. Schülzgen, S. Chen, V. L. Temyanko, J. V. Moloney, and N. Peyghambarian, "Phase locking and in-phase supermode selection in monolithic multicore fiber lasers," Opt. Lett. 31, 2577-2579 (2006)
22. X. Fang, M. Hu, C. Xie, Y. Song, L. Chai, and C. Wang, "High pulse energy mode-locked multicore photonic crystal fiber laser," Opt. Lett., vol. 36, no. 6, pp. 1005-1007, 2011.
23. P. Zhou, X. Wang, Y. Ma, H. Ma, X. Xu and Z. Liu, "Beam Quality and Power Scalability of Various Multicore Fiber Lasers," Chinese Phys. Lett., vol. 26, no. 8, pp. 084205-1-3, 2009.
24. Y. Li and T. Erdogan, "Cladding-mode assisted fiber-to-fiber and fiber-to-free-space coupling," Opt. Commun., vol. 183, no. 5–6, pp. 377-388, 2000.
25. A. E. Siegman, "High-power laser beams: defining, measuring and optimizing transverse beam quality", Proc. SPIE 1810, 9th International Symposium on Gas Flow and Chemical Lasers, (4 May 1993).
26. L. Michaille, C. R. Bennett, D. M. Taylor and T. J. Shepherd, "Multicore Photonic Crystal Fiber Lasers for High Power/Energy Applications," IEEE Journal of Selected Topics in Quantum Electronics, vol. 15, no. 2, pp. 328-336, 2009.